The possible origin of the faint fuzzy star clusters in NGC 1023

M. Fellhauer, P. Kroupa

Institute for Theoretical Physics and Astrophysics, University of Kiel, Germany

mike,pavel@astrophyik.uni-kiel.de

Received _____; accepted _____

ABSTRACT

In the lenticular galaxy NGC 1023 a new population of star clusters ("faint fuzzies") was recently discovered by Larsen & Brodie. These clusters are found inside the disc and are faint ($23 \leq V \leq 24$ mag) and extended with effective radii of $r_{\rm eff} \approx 7$ to 15 pc.

We present here N-body calculations of a likely formation-scenario through merging star clusters in clusters of star clusters (super-clusters). Such super-clusters are observed to form in interacting galaxies.

The resulting merger objects have masses comparable to the "faint fuzzies" and show large effective radii ($r_{\rm eff} > 7$ pc). Even though these objects are suffering from strong tidal forces they are able to survive and reach the estimated ages of the extended star clusters in NGC 1023.

Subject headings: galaxies: star clusters – galaxies: interaction – galaxies: individuals (NGC 1023) – methods: N-body simulations

1. Introduction

During a recent search for globular clusters (GC) in NGC 1023, a lenticular galaxy at approximately 9 Mpc distance, Larsen & Brodie (2000) found faint objects ($23 \leq V \leq 24$ mag) that have GC luminosities but effective radii (= half-light radii) of 7 to 15 pc which is much larger than ordinary GCs that have effective radii of 2 to 3 pc. Using spectra obtained with the Keck telescope they (Brodie & Larsen 2002) confirmed that these objects belong to NGC 1023 and have ages of about ≥ 7 to 8 Gyr, are moderately metal rich ($[{\rm Fe/H}] = -0.58 \pm 0.24$) while showing a super-solar α-element abundance ($[\alpha/{\rm Fe}] = +0.3$ to $+0.6$). While GC are usually connected with the spherical component of a galaxy, these

new objects appear to be situated in the disc of NGC 1023. The distribution of these objects shows rotation around the galaxy. The authors conclude that they have found a new class of star clusters which they call "faint fuzzies".

NGC 1023 has a dwarf companion (NGC 1023A) with which it is steadily interacting, and due to its lenticular appearance it probably suffered from interactions and mergers in the past leading to strong star formation events.

Interactions between gas-rich galaxies lead to strong star formation events. For example, HST-images of the Antennae reveal (Whitmore et al. 1999) that the knots of intense star formation produce clusters of massive young star clusters. These "super-clusters" (= clusters of star clusters; not to be confused with super stellar clusters (SSC), which are individual massive star clusters) appear to contain dozens to hundreds of massive star clusters within a region spanning a few hundred pc to a kpc in diameter.

Here we report N-body results concerning the dynamical evolution of such super-clusters. The resulting merger objects have similar properties as the "faint fuzzies".

2. Simulations

We use the particle-mesh code SUPERBOX (Fellhauer et al. 2000) which incorporates a hierarchical grid architecture allowing high resolution at the places of interest.

We model the single star clusters as Plummer spheres (Plummer 1911, numerical realisation: Aarseth et al. 1974) with a Plummer radius of 4 pc, which corresponds to

the mean half-light radius found for the individual young star clusters in the Antennae (Whitmore et al. 1999). $N_0 = 262$ star clusters with a mass range of $10^4 - 10^6$ $M_\odot$ following a power-law mass spectrum,

$$n(M_{\rm cl}) \quad \propto \quad M_{\rm cl}^{-1.5}, \tag{1}$$

are placed in a Plummer distribution with Plummer radius $r_{\rm pl}^{\rm sc}$ representing the super-cluster. The super-cluster orbits on an eccentric orbit around the host galaxy represented by an analytical potential, which consists of a disc modelled as a Plummer-Kuzmin potential and a spherical halo component modelled as a logarithmic potential:

$$\begin{aligned} \Phi_{\rm gal} &= \Phi_{\rm disc} + \Phi_{\rm halo} \\ &= -\frac{GM_{\rm disc}}{\sqrt{R^2 + (a + \sqrt{z^2 + b^2})^2}} - \frac{1}{2} v_0^2 \ln(R_{\rm gal}^2 + R^2), \end{aligned} \tag{2}$$

with $M_{\rm disc} = 10^{11}$ $M_\odot$, $a = 3$ kpc, $b = 0.3$ kpc, $v_0 = 200$ km/s and $R_{\rm gal} = 50$ kpc which sums up to an almost flat rotation curve with a rotation speed of 220 kms^{-1}.

Several simulations with different values for the scale length $r_{\rm pl}^{\rm sc}$ of the super-cluster, different initial masses $M_{\rm sc}$ of the super-cluster and different orbits around the host galaxy are performed to study the evolution of the resulting merger object. The computational setup closely follows that used in previous studies (Fellhauer et al. 2002; Fellhauer & Kroupa 2002).

It is possible to follow the evolution with a particle-mesh code that neglects dynamical effects of two-body relaxation, because the half-mass (bulk) two-body relaxation times of the single star clusters, which can be estimated by (Binney & Tremaine 1987)

$$t_{\rm relax} = \frac{664}{\ln(0.5N)} \left(\frac{M_{\rm cl}}{10^5 {\rm M}_\odot} \right)^{1/2} \left(\frac{1 {\rm M}_\odot}{\overline{m}} \right) \left(\frac{r_{0.5}}{1 {\rm pc}} \right)^{3/2} {\rm Myr}, \tag{3}$$

is $\approx$ 800 Myr for a 10^4 $M_\odot$ star cluster ranging up to 4.4 Gyr for a 10^6 $M_\odot$ star cluster, while the merging timescale is much shorter (Fellhauer et al. 2002). Furthermore, as shown below, the resulting merger objects have relaxation times of a Hubble-time or longer.

3. Results

In a previous paper (Fellhauer et al. 2002) it was shown that the star clusters inside a super-cluster merge within a few crossing times of the super-cluster (typically 50 to 500 Myr). The resulting merger objects are stable and compact. Their masses range from being similar to GCs, in cases where the tidal field removes a large fraction of the individual clusters leaving merger objects consisting of only a few star clusters. On the other hand, when the super-cluster is sufficiently concentrated and the tidal field is correspondingly weak the merger object evolves to become an ultra-compact dwarf galaxy (UCD) (Fellhauer & Kroupa 2002), a new class of objects discovered recently in the Fornax galaxy cluster (Phillipps et al. 2002; Hilker et al. 1999). To show the different results of a wide range of our simulations we plot the effective radii and the masses of the merger objects as a function of the Plummer radius of the super-cluster (Fig. 1). Even if tidal forces are strong, compact and massive super-clusters evolve into extended objects with lifetimes significantly longer than 5 Gyr although they orbit well inside the disc.

Here we give the results of a simulation (OC03, filled box in Fig. 1) where the super-cluster was placed on an orbit within the galactic disc which accounts for the scenario in NGC 1023. The resulting merger object is far too massive to be one of the "faint fuzzies" found in NGC 1023, rather resembling an object like ω-Cen in our Milky Way but with two additional simulations we show that these results still hold for less massive objects like the faint extended star clusters in NGC 1023.

The super-cluster has initially a Plummer radius of $r_{\rm pl}^{\rm sc} = 50$ pc and a cut-off radius of 250 pc. It contains 262 star clusters following the power law of Eq. 1 with a total mass of 10^7 $M_\odot$. The crossing time of the super-cluster is $t_{\rm cr}^{\rm sc} = 10.4$ Myr and the internal velocity dispersion of the clusters in the super-cluster is $\sigma_{\rm sc} = 15.9$ kms^{-1}. Additionally we choose the sense of rotation of all clusters in the super-cluster to be the same to investigate the resulting rotation-law of the merger object. A super-cluster is expected to rotate if it forms from a contracting and locally differentially rotating inner tidal arm. The super-cluster is placed on an eccentric orbit with perigalacticon at 2.1 kpc and apogalacticon at 7.5 kpc. The orbit is inclined such that the maximum Z-distance from the disc plane is about 2 kpc. The parameters are chosen to be representative of the knots seen to contain many star clusters in the Antennae galaxies (Fellhauer & Kroupa 2002), while the orbital inclination is motivated by the orbit of ω-Cen (Dinescu et al. 1999). A possible link between ω-Cen and merged super-clusters has already been pointed out by Fellhauer & Kroupa (2002).

Within the first 250 Myr a merger object forms with a bound mass of about $3 \cdot 10^6$ $M_\odot$. The half-mass radius of this object is 18 pc and the 90% Lagrangian-radius is of the order of 110 pc at that time. The surface density profile of the merger object follows a shallow power law of $\Sigma \propto r^{-2.5}$ as shown in Fig. 2a. The 3-dimensional central velocity dispersion is $\sigma_{3D} = 21.8$ kms^{-1} (Fig. 3a). It also shows a maximum rotation velocity of about 5 kms^{-1} at a distance of about 12 pc from the centre (Fig. 3a). The bulk relaxation time (Eq. 3) of the merger object is ≈ 50 Gyr which is longer than the age of the universe.

The tidal radius calculated using the equation 7-84 from Binney & Tremaine (1987)

$$r_{\rm tidal}(D) \;=\; \left(\frac{M_{\rm mo}}{3M_{\rm gal}(D)}\right)^{1/3} D, \qquad (4)$$

where D denotes the distance to centre of the galaxy and $M_{\rm gal}(D)$ is the enclosed mass of the galaxy at that distance and $M_{\rm mo}$ is the bound mass of the merger object, is about 84 pc at perigalacticon. Therefore the object becomes tidally shaped and looses mass with every perigalacticon passage. After 5 Gyr of simulation time the merger object has lost about half its mass (Fig. 5a). The central surface density drops down to 7500 $\mathrm{M}_\odot\mathrm{pc}^{-2}$. The profile can be fitted with a King profile with King radius (= effective radius) of 6 pc. An alternative fit is an exponential profile in the inner part ($\Sigma \propto e^{-r/6\mathrm{pc}}$) and a steep power law with $\Sigma \propto r^{-5.5}$ for the outer part (Fig. 2b). The half-mass radius has shrunk down to 11.6 pc, the 90% Lagrangian-radius to 27 pc. The tidal radius is determined to be 68 pc at the last perigalacticon and 127 pc at the actual position. Also the central velocity dispersion and the maximum rotation speed has dropped as shown in Fig. 3b. The bulk relaxation time (following Eq. 3) of the merger object is now $t_{\rm relax} \approx 20$ Gyr.

The two additional simulations have $N_0 = 20$ star clusters initially with masses of 10^4 $\mathrm{M}_\odot$ ($M_{\rm sc} = 2 \times 10^5$ $\mathrm{M}_\odot$) (OC07) and 5×10^4 $\mathrm{M}_\odot$ ($M_{\rm sc} = 10^6$ $\mathrm{M}_\odot$) (OC08) respectively. The Plummer-radii of the super-clusters are chosen to be 20 pc. The orbits of the super-clusters have the same eccentricity as in the first simulation but are placed in the X-Y-plane of the galaxy instead of being inclined.

In the OC07 simulation a merger object containing 14 out of the initial 20 star clusters develops after 100 Myr. After 5 Gyr this merger object has a bound mass of $1.8 \cdot 10^4$ $\mathrm{M}_\odot$ (Fig. 5a) and a tidal radius of 24 pc. It's surface density profile can be fitted with a King profile with a central surface density of 240 $\mathrm{M}_\odot\mathrm{pc}^{-2}$ and a King radius (which corresponds to the effective radius) of 5.9 pc. Fitting an exponential profile to the inner part gives $\Sigma_{\rm exp} = 250$ $\mathrm{M}_\odot\mathrm{pc}^{-2}$ and an exponential scale length of about 4 pc. The outer part can

again be fitted with a steep power law $\Sigma \propto r^{-5.9}$ (Fig. 4a). The central line-of-sight velocity dispersion is 1.4 kms^{-1}.

The OC08 simulation shows a merger object which developed out of 18 star clusters. Again the merging process is finished after about 100 Myr. The mass of the merger object after 5 Gyr is $4 \cdot 10^5$ $\mathrm{M}_\odot$ (Fig. 5a) and the tidal radius is 70 pc. Fitting a King profile to the surface density distribution (Fig. 4b) gives the following values: central surface density of 1500 $\mathrm{M}_\odot\mathrm{pc}^{-2}$ and an effective radius of 7.5 pc. The exponential fit has the values 1400 $\mathrm{M}_\odot\mathrm{pc}^{-2}$ and $r_{\mathrm{exp}} = 7.5$ pc. The power law fit to the outer part has an power-law index of -6.0.

The above results (total mass and central surface density) can be converted to total blue luminosity and central surface brightness using mass-to-light ratios taken from a single stellar population model of STARBURST99 (Leitherer et al. 1999). The programme adopts a Salpeter IMF. Therefore, we choose a minimum stellar mass of 0.3 $\mathrm{M}_\odot$ and a maximum mass of 100 $\mathrm{M}_\odot$. Note that we truncate the Salpeter IMF at 0.3 $\mathrm{M}_\odot$. This roughly accounts for the flattening of the IMF below 0.5 $\mathrm{M}_\odot$ (Kroupa 2002). The evolution of M/L_B with time is shown in Fig. 5b as obtained as a result of stellar evolution from STARBURST99. We stop the photometric evolution from STARBURST99 when $M/L_B = 3.0$ is reached because STARBURST99 overestimates the M/L at high ages quite substantially. Instead we take a linear fading with time as proposed by the models of Bruzual & Charlot (1993) of 2 magnitudes from 3 to 15 Gyr. This enables us to place the evolutionary track of our merger objects into a central surface brightness, $\mu_{0,\mathrm{B}}$, vs absolute photometric B-band magnitude, M_{B}, diagram (the Kormendy diagram; Fig. 6). The endpoint of the evolution of our merger objects is also the region where the "faint fuzzies" are located. The faint fuzzies have total

luminosities of about $M_V = -7$ (Larsen & Brodie 2002). We estimate their location in the Kormendy diagram in the following way. First we set $M_V + 1.0 = M_B$ (i.e. adopting $(B - V) = 1.0$ as an admissible approximation for the diagram) then we convert the total luminosity into a total mass using $M/L = 3.0$. With this mass we calculate the tidal radius in our model potential and orbit ($r_{\rm tidal} \approx 50$ pc) and adopt an effective (or King-) radius of 10 pc. Using a King profile we estimate the central surface brightness to be $\mu_{0,B} \approx 22.3$ mag.

4. Conclusions

S0 (lenticular) galaxies are commonly believed to have suffered from interactions with other galaxies which transformed their morphology from a late-type spiral into their early-type form (Kennicutt 1998; Abraham & van den Bergh 2001). Therefore the type of NGC 1023 tells us that this galaxy suffered maybe several but at least one strong interaction (merger) with another galaxy. As is seen in interacting galaxies these events lead to an enhanced star formation activity and to an enhanced rate of super nova explosions of massive stars which accounts for the super-solar enhancement of α-elements. Many of the new stars mostly form in star clusters which are also grouped in super-clusters, as is demonstrated by the Antennae and Stephan's Quintet (Gallagher et al. 2001). These super-clusters are bound entities and form, through successive mergers of their constituent star clusters, new objects which are larger than ordinary GCs. Our simulations show that even strong tidal fields are not able to destroy these objects and they survive for a Hubble-time.

The "faint fuzzies" found in NGC 1023 may have therefore formed as super-clusters during the interactions and the resulting star bursts that shaped NGC 1023. Like in

the Antennae the super-clusters were born within the galaxy and not in the outer tidal tails. Therefore the "faint fuzzies", which one can call extended globular clusters or small ultra-compact dwarf galaxies by virtue of their long two-body relaxation time, stay within the optically visible galaxy and show a similar rotation pattern like the disc. These objects can be old because they are able to survive until the present, they may be rotating and have different populations of stars if old field stars were captured by the young super-cluster.

Given the ubiquity of young super-clusters in the Antennae and Stephan's Quintet, it appears reasonable to expect that such objects form whenever strong star bursts occur. It is therefore exciting, but retrospectively not very surprising, that "faint fuzzies" were discovered in a lenticular galaxy.

Super-clusters that form in outer tidal tails may leave the mother galaxy either by being ejected by the merging galaxies or become unbound due to a tidal field from the galaxy cluster. Such merger objects will appear similar to the UCDs in Fornax (Fig. 7). A related object may be ω-Cen in our Milky Way, which is quite different and more massive than the other GCs. It incorporates at least two different populations of stars and shows a rotation-law resembling that of our merger object (Freeman 2001). ω-Cen is quite old and could therefore be a relic of a star-burst during the formation of the Milky Way. We are investigating the hypothesis that ω-Cen may also be related to super-clusters. Fig. 7 summarises in a schematic way the possible evolutionary paths and resulting objects that may form under this hypothesis.

MF acknowledges financial support through DFG-grant FE564/1-1. MF also acknowledges the support of the European Commission through grant number HPRI-1999-CT-00026 (the TRACS programme at EPCC).

REFERENCES

Aarseth, S.J., Henon, M., & Wielen, R. 1974, A&A, **37**, 183

Abraham, R.G., & van den Bergh, S. 2001, Science, **293**, 1273

Binney, J., & Tremaine, S. 1987, Galactic Dynamics, Princeton Series in Astrophysics, (Princeton, New Jersey: Princeton University Press)

Brodie, J.P., & Larsen, S.S. 2002, AJ, submitted (astro-ph/0203454)

Bruzual, G.A., & Charlot, S. 1993, ApJ, **405**, 538

Dinescu, D.I., van Altena, W.F., Girard, T.M., & Lopez, C.E. 1999, AJ, **117**, 277

Fellhauer, M., Kroupa, P., Baumgardt, H., Bien, R., Boily, C.M., Spurzem, R., & Wassmer, N. 2000, NewA, **5**, 305

Fellhauer, M., Baumgardt, H., Kroupa, P., & Spurzem, R. 2002, Cel.Mech.&Dyn.Astron., **82**, 113

Fellhauer, M., & Kroupa, P. 2002, MNRAS, **330**, 642

Ferguson, H.C., & Binggeli, B. 1994, A&A Rev., **6**, 67

Freeman, K.C. 2001, in ASP Conf. Ser. **228**, Star2000: The dynamics of star clusters and the Milky Way, ed. S. Deiters, B. Fuchs, A. Just, R. Spurzem, R. Wielen (San Francisco, California: ASP), 43

Gallagher, S.C., Charlton, J.C., Hunsberger, S.D., Zaritsky, D., & Whitmore, B.C. 2001, AJ, **122**, 163

Harris, W.E. 1996, AJ, **112**, 1487

Hilker, M., Infante, L., Kissler-Patig, M., & Richtler, T. 1999, A&AS, **134**, 75

Kennicutt Jr., R.C. 1998, AR&A, **36**, 189

Kroupa, P. 1998, MNRAS, **300**, 200

Kroupa, P. 2002, Science, **295**, 82

Larsen, S.S., & Brodie, J.P. 2000, AJ, **120**, 2938

Leitherer, C., Schaerer, D., Goldader, J.D., Delgado, R.M.G., Robert, C., Kune, D.F., de Mello, D.F., Devost, D., & Heckman, T.M. 1999, ApJS, **123**, 3

Mateo, M. 1998, ARAA, **36**, 435

Pelletier, R.F., Davies, R.L., Illingworth, G.D., Davies, L.E., & Cawson, M. 1990, AJ, **100**, 1091

Phillipps, S., Drinkwater, M.J., Gregg, M.D., & Jones, J.B. 2001, ApJ, **560**, 201

Plummer, H.C. 1911, MNRAS, **71**, 460

Whitmore, B.C., Zhang, Q., Leitherer, C., & Fall, S.M. 1999, AJ, **118**, 1551

This manuscript was prepared with the AAS LaTeX macros v5.0.

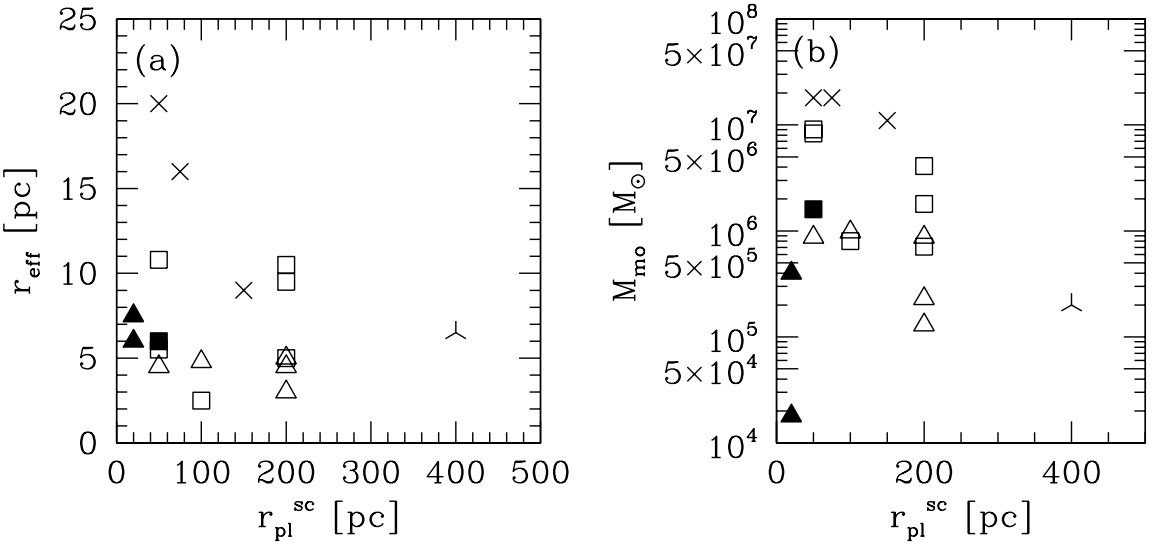

Fig. 1.— Effective radii, $r_{\rm eff}$, (a) and masses, $M_{\rm mo}$, (b) of our merger objects evaluated at 5 Gyr vs. Plummer radius of the initial super-cluster $r_{\rm pl}^{\rm sc}$. Crosses: large initial super-cluster mass ($M_{\rm sc} \geq 10^7$ M$_\odot$) and weak tidal field (distance at perigalacticon $R_{\rm peri} \geq 10$ kpc); boxes: large mass and strong tidal field (distance at apogalacticon $R_{\rm apo} < 10$ kpc); triangles: low mass ($M_{\rm sc} < 10^7$ M$_\odot$) and strong tidal field; tri-pointed stars: low mass and weak tidal field. Filled symbols show the models discussed in the paper.

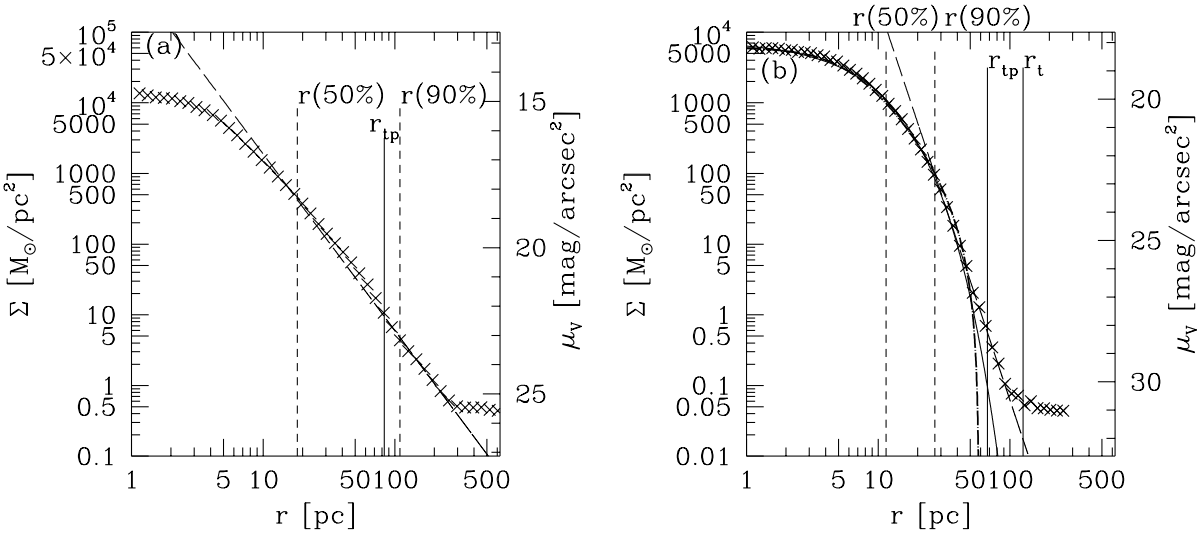

Fig. 2.— Projected surface density profile of the merger object. The vertical lines are as follows: dashed: half-mass and 90%-Lagrangian radius; solid: tidal radius at the position of the merger object (r_t) and at the last perigalacticon ($r_{t,p}$). (a): Measured at $t = 350$ Myr (shortly after formation of the merger object). The dashed line is a power law with $\Sigma \propto r^{-2.5}$. The adopted mass-to-light ratio to calculate the surface-brightness is 0.3. (b): Profile at $t = 5$ Gyr. Dot-dashed line shows the fitted King profile, solid line is the exponential fit for the inner part and dashed line is the fitted power law for the outer part. The adopted mass-to-light ratio is 3.

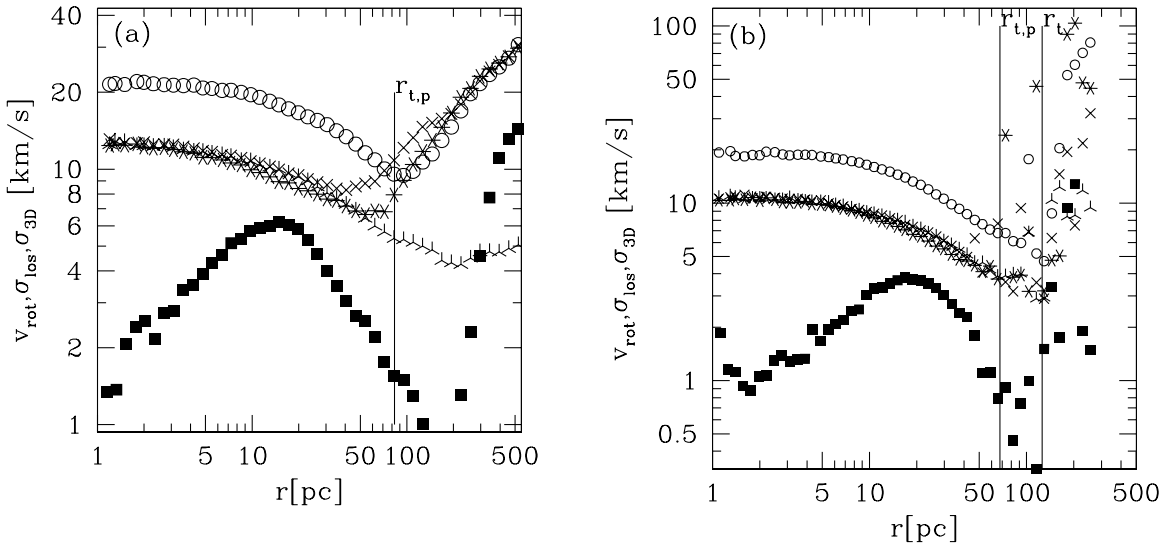

Fig. 3.— Velocity distribution in the merger object; circles show the 3-dimensional velocity dispersion computed in concentric shells around the centre; three-, four- and six-pointed stars are the projected line-of-sight velocity dispersions along the x-, y- and z-coordinate axis evaluated in concentric rings. Squares show the mean rotational velocity again measured in concentric shells. Note the similarities to the rotation-law observed for ω-Cen (Freeman 2001). Vertical line shows the tidal radius at perigalacticon. (a): Measured at $t = 350$ Myr (shortly after formation of the merger object). (b): Distributions at $t = 5$ Gyr.

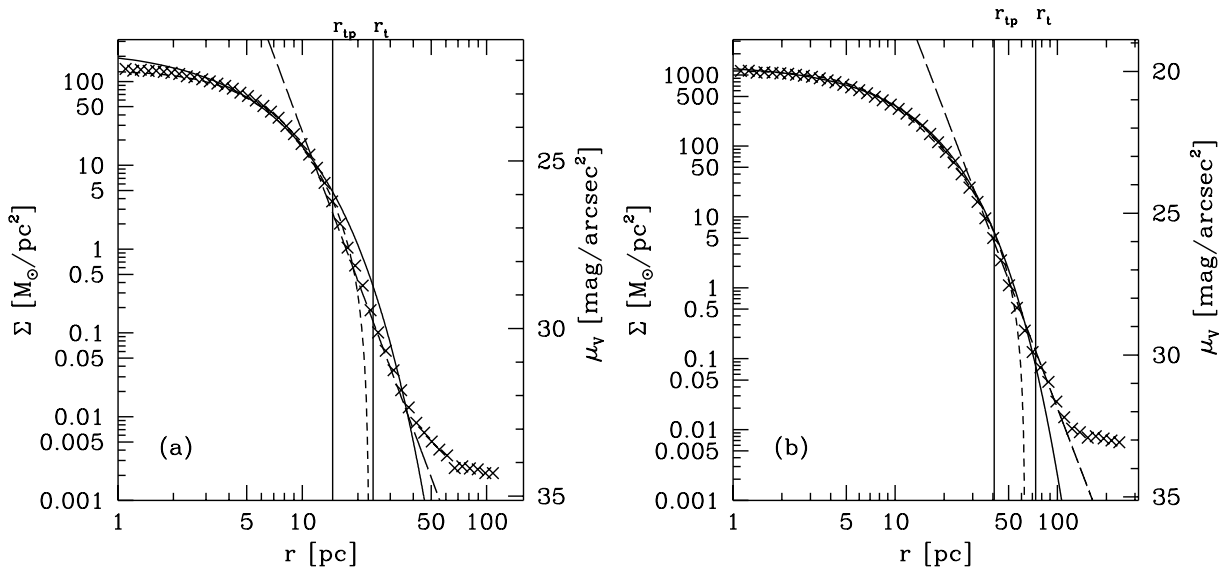

Fig. 4.— Projected surface density profile of the merger objects. The vertical lines are the calculated tidal radii at perigalacticon ($r_{t,p}$) and at the actual distance (r_t) (at $t = 5$ Gyr) of the merger objects. The solid curves show the fitted exponential profiles, the short dashed the fitted King profile and the long dashed the fitted power law with the values according to the main text. (a) OC07: Simulation with $M_{\rm sc} = 2 \cdot 10^5$ M$_\odot$; (b) OC08: Simulation with $M_{\rm sc} = 10^6$ M$_\odot$.

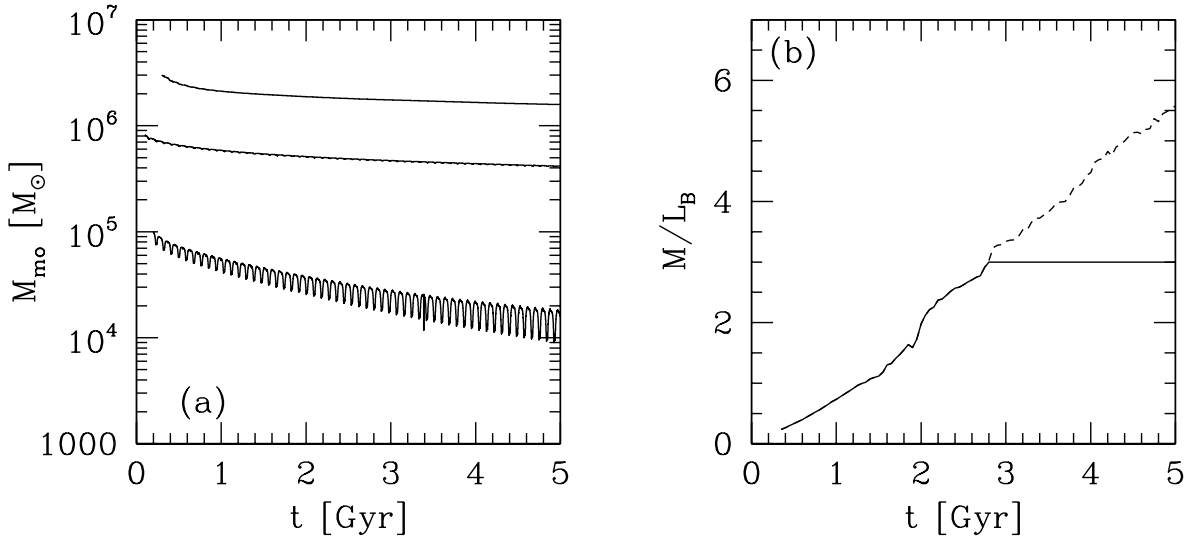

Fig. 5.— (a): Mass of the merger objects vs. time. From top to bottom: $M_{\rm sc} = 10^7$ $M_\odot$ (OC03), $M_{\rm sc} = 10^6$ $M_\odot$ (OC08) and $M_{\rm sc} = 2 \cdot 10^5$ $M_\odot$ (OC07). (b): Evolution of the mass-to-light ratio M/L_B taken from STARBURST99 (dashed line) and the "frozen" value ($M/L_B = 3.0$) used to calculate the luminosities (solid line).

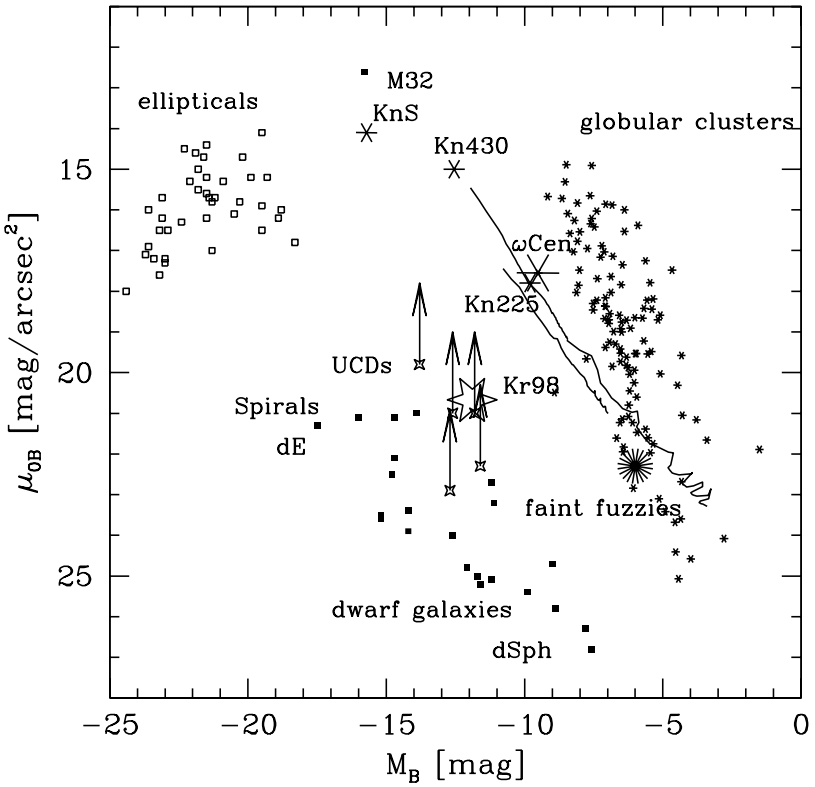

Fig. 6.— Central surface brightness, $\mu_{0,\mathrm{B}}$, vs absolute photometric B-band magnitude, M_B (the Kormendy diagram). The stars are data for Milky-Way globular clusters (GC, Harris 1996), Local-Group dwarf galaxies (Mateo 1998) are displayed as filled boxes, elliptical galaxies (E, Peletier et al. 1990) are shown as open boxes. The positions of disk galaxies are indicated by "Spirals" (cf. Ferguson & Binggeli 1994). The newly discovered UCDs are shown by arrows with lower-limits on μ_B (Phillipps et al. 2001). Three "knots", (KnS, Kn430, Kn225, tables 1 and 2 in Whitmore et al. 1999), observed in the interacting Antennae galaxies are shown as stars. Knots KnS and Kn430 are roughly 10 Myr old so that $M/L_\mathrm{B} \approx 0.035$, while Kn225 is about 500 Myr old ($M/L_\mathrm{B} \approx 0.476$). The open six-pointed star symbol shows the merged super-clusters predicted by Kroupa (1998) to result from the dynamical evolution of such knots, which consist of dozens to hundreds of young star clusters. The large fuzzy symbol shows the approximate location of the faint fuzzy star clusters. The lines show the evolution of our merger objects from the time of formation until 5 Gyr using M/L_B from Fig. 5b and an additional linear fading for ages > 3 Gyr (from top-left to bottom-right: OC03, OC08 and OC07).

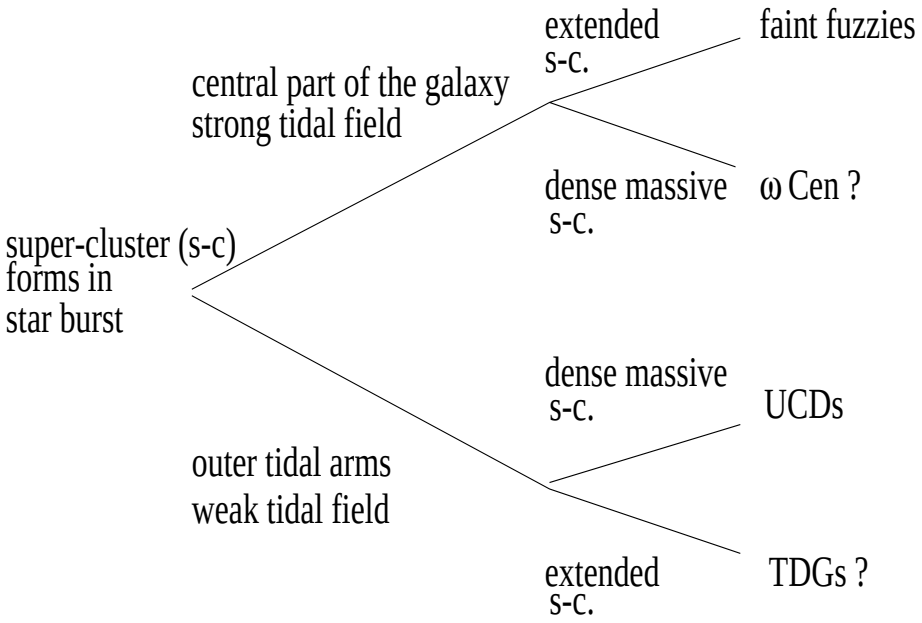

Fig. 7.— Schematic of possible evolutionary tracks of super-clusters. Question marks signify on-going research.